

First Spitzer Space Telescope Observations of Magnetic Cataclysmic Variables: Evidence for Excess Emission at 3–8 microns

Steve B. Howell,¹ Carolyn Brinkworth,² D. W. Hoard,² Stefanie Wachter,² Thomas Harrison,³ Howard Chun,^{4,7} Beth Thomas,^{4,8} Linda Stefaniak,^{4,9} David R. Ciardi,⁵ Paula Szkody,⁶ Gerard van Belle⁵

ABSTRACT

We present the first observations of magnetic cataclysmic variables with the Spitzer Space Telescope. We used the Infrared Array Camera to obtain photometry of the polars EF Eri, GG Leo, V347 Pav, and RX J0154.0-5947 at 3.6, 4.5, 5.8, and 8.0 μm . In all of our targets, we detect excess mid-infrared emission over that expected from the component stars alone. We explore the origin of this IR excess by examining bremsstrahlung, cyclotron emission, circumbinary dust, and L/T brown dwarf secondary stars. Bremsstrahlung and cyclotron emission appear unlikely to be significant contributors to the observed fluxes. At present, the most likely candidate for the excess emission is dust that is probably located in a circumbinary disk with an inner temperature near 800 K. However, a simple dust disk plus any reasonable low mass or brown dwarf-like secondary star is unable to fully explain the observed flux densities in the 3–8 μm region.

¹WIYN Observatory and National Optical Astronomy Observatory, 950 N. Cherry Ave., Tucson, AZ 85719 *howell@noao.edu*

²Spitzer Science Center, California Institute of Technology, Pasadena, CA 91125

³Dept. of Astronomy, New Mexico State University, Box 30001, MSC 4500, Las Cruces, NM 88003

⁴NASA/NOAO Spitzer Space Telescope Observing Program for Students and Teachers

⁵Michelson Science Center, California Institute of Technology, Pasadena, CA 91125

⁶Dept. of Astronomy, University of Washington, Box 351580, Seattle, WA 98195

⁷Cranston High School East, 899 Park Ave., Cranston, RI 02910

⁸Environmental Education, Great Falls Public Schools, West Elementary, 1205 1st Ave. NW, Great Falls, MT 59404

⁹Allentown High School, 27 High Street, Allentown, NJ 08501

Subject headings: Stars: individual (EF Eri, GG Leo, V347 Pav, RX J0154.0-5947) — stars: low-mass — stars: brown dwarfs

1. Introduction

Cataclysmic variables (CVs) are interacting binary stars containing a white dwarf (WD) primary and a low mass secondary (Warner 1995). CVs that contain a highly magnetic WD, with surface fields ranging from 10–250 MG, are called polars. In a polar, accreted material flows along magnetic field lines, does not form a viscous disk, and accretes directly onto the WD at/near its magnetic pole(s). Polars are well known to stop and (re)start their mass transfer, causing changes of ~ 2 –3 (or more) optical magnitudes at apparently random intervals. During low states, the accretion flux disappears and the two component stars can often be cleanly observed. For the past few decades, theoretical models of CV evolution (Kolb 1993; Howell et al. 2001) have predicted that the very shortest orbital period systems should contain low mass, brown dwarf-like secondary stars. More recently, near-IR (*JHK*) observations of the shortest period CVs (e.g., Harrison et al. 2003; Howell et al. 2004) have provided evidence that they likely do contain secondaries similar to L or T dwarfs.

We have accomplished an initial survey of four polars (EF Eridani, GG Leonis, V347 Pavonis, and RX J0154.0-5947) using the Infrared Array Camera (IRAC) on the Spitzer Space Telescope. We specifically chose ultra-short period polars ($P_{\text{orb}} \leq 90$ min) to facilitate studying the brown dwarf-like secondary stars predicted to be present. We found that all four of the polars show emission in the 3–8 μm region in excess of that produced solely by the WD plus an M or L dwarf. In this Letter, we briefly discuss our observations and possible sources of this excess emission. The best explanation is cool circumbinary dust that would likely dynamically settle into a disk, and/or possibly a T dwarf-like secondary star.

2. Spitzer Infrared Array Camera Observations

IRAC is a four channel camera that obtains nearly simultaneous images at 3.6, 4.5, 5.8, and 8.0 μm (see Fazio et al. 2005). For our polars, we obtained 30-sec images using the Gaussian-5 dither pattern. The dithered images were combined and flux calibrated with the S12 Spitzer pipeline. Details of our data reduction and error analysis procedures will be presented in Brinkworth et al. (2006). Figure 1 shows the spectral energy distributions (SEDs) for our polars, comprised of our IRAC data (Table 1) and non-simultaneous 2MASS *JHK_s* photometry. We have classified the polars based on the overall appearance of their

JHK_s SEDs. EF Eri was known to be in a low accretion state during its 2MASS observation (Harrison et al. 2004), and we infer that V347 Pav was also, based on its similar SED. We suspect that GG Leo and RX J0154 were both in high accretion states during their 2MASS observations, because of the falling Rayleigh-Jeans (RJ) tail of accretion flux that dominates their JHK_s SEDs. We note that the 2MASS bands are sensitive to the mass accretion state of the system (high states show a falling RJ tail, low states probably begin to reveal the secondary star) while the IRAC bands are red enough to be essentially unaffected by these changes.

3. Source of the Excess 3–8 micron Emission

Our Spitzer observations show that all four polars present a similar, relatively flat SED in the IRAC region. The 3–8 μm emission does not fall off to the red as it would if the source was a hot blackbody or the stellar RJ tail of an M or L star. We now examine some possibilities for its origin.

3.1. Cyclotron Emission

The high magnetic fields in polars can produce cyclotron emission in the UV–near-IR spectral regions as accreted material is ionized and the free electrons spiral along field lines (Warner 1995). At times, cyclotron cooling can become the dominant cooling mechanism (Cropper 1990) and its blue spectrum consists of large hump features $\sim 1000\text{\AA}$ wide that can increase the local continuum by up to one magnitude. A thorough review of model cyclotron spectra is given in Wickramasinghe & Ferrario (2000, hereafter WF2000). Spectral intensity and shape, as well as any harmonic structures (humps), are dependent on magnetic field strength, electron temperature and density, and viewing angle. Cyclotron spectra are characterized by a long wavelength RJ tail and a slowly rising, power-law blue continuum modulated by harmonic hump features. The peak of this pseudo-blackbody spectrum moves blueward as the magnetic field strength increases (e.g., Fig. 32 in WF2000).

Fields of 14–30 MG, as found in our target polars (Warner 1995), produce power law continua and observable humps in the optical–near-IR spectral region, with optically thick RJ tails at longer wavelengths. If we (incorrectly) attribute all the K_s band flux in EF Eri to the RJ tail of cyclotron emission, then we would expect the IRAC observations to produce flux densities of ≈ 114 , 58, and 38 μJy at 4, 6, and 8 μm , respectively. This is not consistent with our observations. In order for the cyclotron spectrum alone to produce a relatively

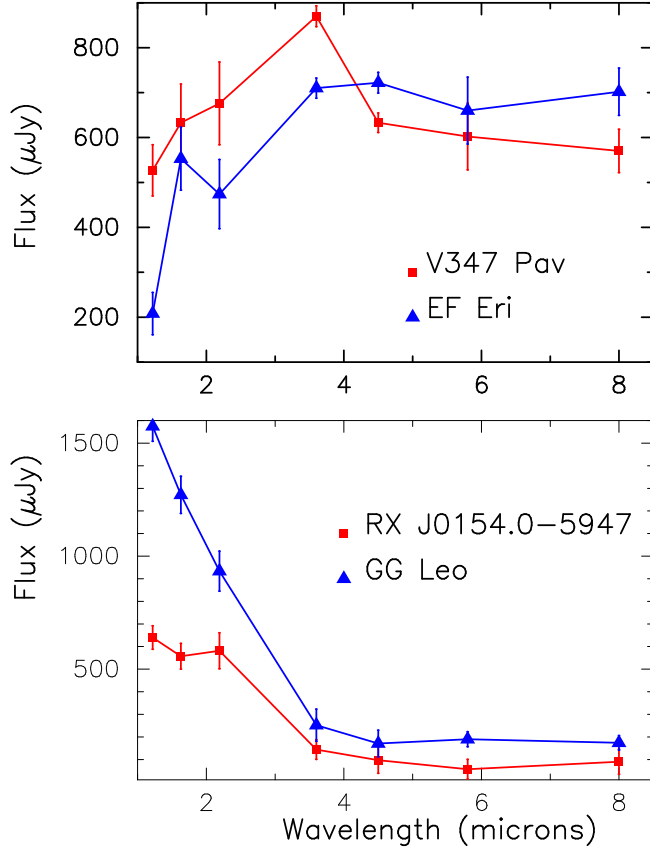


Fig. 1.— Spitzer IRAC photometric observations at 3.6, 4.5, 5.8, and 8.0 μm and 2MASS JHK_s photometry for the polars EF Eri and V347 Pav (top) and GG Leo and RX J0154.0-5947 (bottom).

Table 1. 2MASS and Spitzer IRAC Fluxes (μJy)

Polar	1.2 μm	1.6 μm	2.2 μm	3.6 μm	4.5 μm	5.8 μm	8.0 μm
EF Eri	208(47)	553(70)	474(77)	710(22)	722(23)	660(74)	702(53)
V347 Pav	527(57)	633(86)	676(92)	870(23)	633(22)	602(74)	570(48)
GG Leo	1575(66)	1272(82)	933(88)	252(71)	170(59)	190(33)	174(32)
RX J0154 ^a	640(52)	557(57)	581(80)	144(43)	97(58)	57(43)	91(55)

^aRX J0154 is our faintest target in the IRAC bands; however, it was clearly detected in each IRAC channel. Our formal 1σ errors for this star, as listed in the table, are probably best taken as lower limits.

flat SED in the 3–8 μm region, the IRAC observations would have to sample the power-law portion (plus humps). This would require magnetic field strengths of only a few MG, which may be found in polars at large distances from the WD ($B \propto r^{-3}$). Fields of 1–2 MG occur at about 2–3 WD radii in our polars, assuming conservation of magnetic flux density. At the same viewing geometry and opacity, the emission volume in this low field region will be larger than at the accretion pole by a factor $(r/R_{\text{WD}})^3$, but the electron temperature and material density will be lower.

The ratio of overall spectral intensity from the low field region (I_r) compared to the pole region (I_R) is proportional to

$$I_r/I_{R_{\text{WD}}} \propto (B_r/B_{\text{WD}})(r/R_{\text{WD}})^3 N_e T_e e^{-(r/R_{\text{WD}})} \approx 0.07,$$

(see Eqn. 53 in WF2000) where $N_e \sim 10^{14} \text{ cm}^{-3}$ and $T_e \sim 5 \text{ keV}$, typical low state values at the magnetic pole on the WD surface. If we assign all the 3.6 μJy flux in EF Eri (711 μJy) to cyclotron emission from the main field, then weak field cyclotron radiation would produce a flat SED of only $\sim 50 \mu\text{Jy}$ across the IRAC bands. This is much fainter than our Spitzer data, but is in agreement with recent limits set by non-detection of cyclotron emission in Spitzer observations of intermediate polars (Johnson et al. 2005), which are believed to have WD surface fields of a few MG. Thus, it seems that any cyclotron emission present in the IRAC bands would provide only a small addition to the observed flux, possibly as a low level RJ tail, and cannot, in itself, account for the observed shape or level of the 3–8 μm SED in our polars.

3.2. Bremsstrahlung

Bremsstrahlung, or free-free emission, produces a flat SED and can be the dominant continuum source at radio wavelengths or in high temperature environments. The total energy (in ergs) radiated per cm^3 per second for a pure hydrogen environment is given by

$$E_{\text{ff}} = 1.4 \times 10^{-27} N_e^2 T^{0.5} \langle g \rangle,$$

where $\langle g \rangle$, the Gaunt factor, is near 1 (Spitzer 1978). Bremsstrahlung is nearly independent of frequency until its cutoff frequency, a value set by the electron thermal velocity distribution (i.e., $h\nu \approx kT$). At high temperatures ($\gg 10^6 \text{ K}$) this cutoff frequency is in the optical–IR, while lower temperatures only produce significant bremsstrahlung in the radio.

At typical electron densities ($N_e \sim 10^{13} \text{ cm}^{-3}$) and high state temperatures (100,000–600,000 K) near the WD pole(s) (Warner 1995), and assuming an emission region of 0.1 of the WD area, $E_{\text{ff}} \sim 2600 \text{ erg s}^{-1}$. Over the IRAC bands, even such high temperature regions

would provide a continuum level of only about $10^{-10} \mu\text{Jy}$. This is $\sim 10^{13}$ less than expected from the RJ tail of a 1500 K star at the distances of our polars (Rybicki & Lightman 1979). Looking instead at low temperature environments within the CV, a temperature of only ~ 3600 K will produce a cutoff frequency at $4 \mu\text{m}$. However, the number density of free electrons continuously kept at this temperature, which is required to produce measurable bremsstrahlung in the IRAC bands, must exceed 10^{15} cm^{-3} . This is a highly unrealistic value – it would require the total accumulated mass of many thousands of years of high state mass transfer ($10^{-12} M_{\odot} \text{ yr}^{-1}$) between the two stars. In order to lower the number density of 3600 K material to even a remotely plausible value of 10^{11} cm^{-3} , a spherical radiating volume with radius near 10^{15} cm is needed. This is about 100,000 times the size of the binary orbit. We can, therefore, likely eliminate bremsstrahlung as the sole or major source of the observed IR SEDs in our polars.

3.3. Circumbinary Dust

An interesting theoretical concept has been pursued of late (e.g., Taam & Spruit 2001) that predicts the existence of circumbinary disks of cool material in CVs. Observational studies to find such disks have provided mixed results (Belle et al. 2004; Dubus et al. 2004) and, to date, there is little direct observational evidence for their existence.

Becklin et al. (2005) present observations of a dust disk surrounding GD362, a single, cool ($T = 9740$ K) WD. In Figure 2, we show the SEDs for EF Eri and V347 Pav (from Figure 1) with the optical–near-IR model of Harrison et al. (2003) plus the Becklin et al. model dust disk, scaled to the distance of EF Eri (45 pc). The Harrison et al. model for EF Eri spans 3500\AA to the K band and is based on actual observations of the cool ($T = 9500$ K) WD, and near-IR photometry and spectroscopy that led to a best-fit secondary approximating the SED of an L8 star. Note the negligible contribution from the WD in EF Eri seen in the extreme lower left corner of Figure 2. This illustrates the steepness of a stellar RJ tail. The Becklin et al. dust disk with $T_{\text{inner}} = 1200$ K is likely to be too hot for our polars, as the inner edge of the circumbinary disk will be farther from the WD. Scaling the inner edge of the disk in GD362 to that in our binaries (assuming the inner edge must be outside the two stars) we find that T_{inner} would be near 800 ± 200 K. This cooler disk model is also plotted in Figure 2. The dust disk model does a fairly good job of fitting the polar SEDs up to $\sim 5 \mu\text{m}$ but then rises too fast toward the red. The cooler 800 K model fits better but is still too bright in the longest IRAC band. The dust disk scaling performed here, and the better fit afforded by the cooler disk, are simple ad hoc models at present. Detailed, more realistic dust disk models are being produced and will be presented in Brinkworth et al. (2006).

3.4. L or T Dwarf Secondary Stars

We compared the SEDs of EF Eri and V347 Pav to those of single L and T dwarfs from the IRAC observed sample kindly provided by Patten et al. (2006). The polar secondary stars have attained their present size, mass, and temperature after Gyr of mass loss; hence, they are brown dwarf-like but are unlikely to be exactly like brown dwarfs. The SED of an L6 dwarf falls off after $4.5\ \mu\text{m}$ (dropping by a factor of 2 in brightness from 4.5 to $8\ \mu\text{m}$), while the SEDs of late T dwarfs remain relatively flat throughout the IRAC bands. We conclude that T dwarf SEDs are more consistent than those of L dwarfs with our observed spectral shapes in the IRAC bands, but neither type of star reproduces the observations in detail. In particular, T dwarfs are quite faint, and would require the CVs to be at very small distances in order to contribute a large fraction of the observed IRAC flux densities. For example, if the IRAC fluxes were entirely due to the secondary star, EF Eri would have to be at ≈ 12 and ≈ 6 pc if the secondary star were a T6.0 and T8.0 respectively.

4. Discussion and Summary

Figure 3 shows an IRAC two-color diagram for our polars, along with several brown dwarfs from the Patten et al. sample (L6 = SDSS 1331-0116; T5 = 2MASS 0559-1404; T8 = 2MASS 0415-0935). We have also plotted GD1400, a detached WD+L5/6 binary with no dust (Farihi et al. 2006), and our simple dust disk model (based on GD362), as shown in Figure 2. The effect of changing the GD362 model disk temperature from $T_{\text{inner}} = 1200$ K to 800 K is shown in the lower right of the figure. For comparison, the IRAC colors of T Leonis and VY Aquarii are also plotted; these are not-yet-published CVs that we have observed with Spitzer. They have similar orbital periods and distances as our polars, but contain non-magnetic WDs surrounded by hot (~ 8000 K) accretion disks. The SEDs of T Leo and VY Aqr are dominated by the RJ tails of the secondary star and accretion disk well into the IRAC region. Our observed polars occupy a region of color-space intermediate between WD+brown dwarf binaries without dust, single brown dwarfs, and dust disk-dominated systems.

Bremsstrahlung, while often producing a flat spectral continuum, likely contributes essentially nothing to our observed IRAC fluxes. Cyclotron emission also appears unlikely to be a major contributor to the SEDs of our polars, since it should be present only as a low level falling RJ tail. However, our understanding of the complex nature of cyclotron emission is far from perfect, so we hesitate to say with complete certainty that none of the excess emission is due to the cyclotron process. At present, the best candidates for the origin of the observed IR excess are cool dust (in or near the CV) and/or secondary stars that are

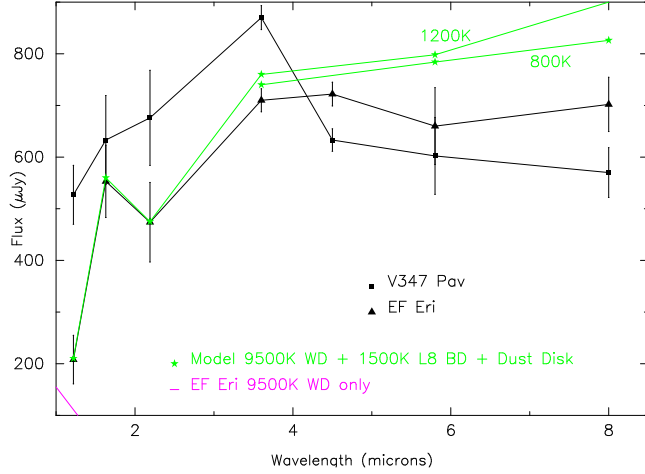


Fig. 2.— The SEDs of EF Eri and V347 Pav from Figure 1 with model SEDs (green lines) based on optical–near-IR observations of EF Eri plus a dust disk based on observations of GD362 (see text for details). The WD-only contribution in EF Eri is shown in the extreme lower left (purple line).

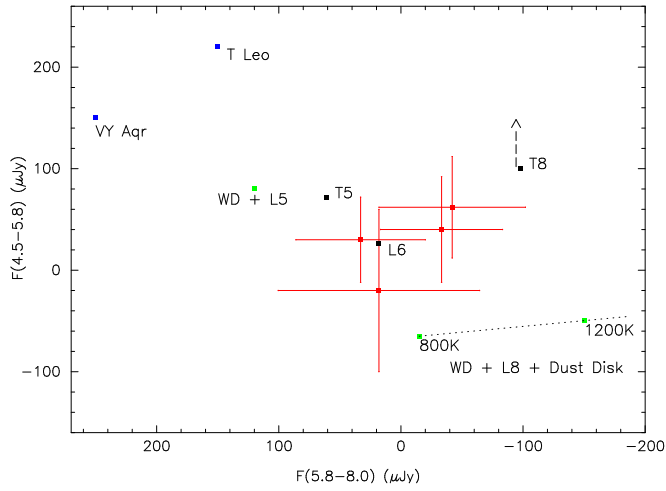


Fig. 3.— IRAC color-color diagram showing our four polars (red points with error bars). The WD+L5 green point is GD1400 (Farihi et al. 2006) and the two green points at 800K and 1200K, represent our scaled GD362 (WD+L8) dust disk model as described in §3.3. The white points are observed single L6, T5, and T8 dwarfs, and the two blue points are observed accretion disk dominated CVs (T Leo and VY Aqr). The $F(4.5–5.8)$ value for the T8 dwarf is off scale at $1384 \mu\text{Jy}$ as indicated by the arrow in the figure. See the text for details.

similar to late T dwarfs.

If the dust is produced by aeons of mass outflow from the CV (in winds or nova outbursts) or is possibly remnant material from the common envelope stage ejected with some orbital angular momentum (e.g., Hinkle et al. 2006), then dynamic considerations lead us to expect that this material would settle into a circumbinary disk. If a dust disk is present and is similar to that seen around GD362, then we expect the inner disk temperature to be around 800 K. The emitting volume of such a disk must be large compared to the component stars (which are Earth-sized and Jupiter-sized), as it outshines even the cool brown dwarf-like secondary in the IRAC bands. If the 3–8 μm SED originates primarily from the secondary star, then it would have to be similar to a late T dwarf and these CVs would have to be far closer than observations of their WDs suggest.

The likely presence of a circumbinary dust disk in polars naturally leads us to postulate that such disks might be common in other CVs. The 3–8 μm region still contains a strong spectral contribution from the RJ tail of the accretion disk in CVs with weakly- or non-magnetic WDs. In longer period systems, the larger, brighter G, K, and early M secondary stars also contribute in the IRAC bandpass. Thus, the contrast from the weak IR emission of a dust disk against that produced by the stellar and other components in all but the polars may prevent detection shortward of 8 μm . Some support for this is provided by Dubus et al. (2004), who detected SS Cygni and AE Aquarii at 11 and 17 μm , and by Abada-Simon et al. (2005), who detected AE Aqr at wavelengths out to 170 μm ¹.

Neither a simple dust disk, as described here, nor a brown dwarf-like secondary star alone can fully explain the observed IR excess in the polars, especially redward of ≈ 6 μm . Spectral observations would help distinguish between the possibilities discussed above and provide details regarding the cause of the observed IR excess.

This work is based on observations made with the Spitzer Space Telescope, which is operated by the Jet Propulsion Laboratory, Caltech, under NASA contracts 1407 and 960785. We thank the Spitzer Science Center (SSC) Director for his generous allocation of observing time for the NASA/NOAO Spitzer Space Telescope Observing Program for Students and Teachers. NOAO, which is operated by the Association of Universities for Research in Astronomy (AURA), Inc., under cooperative agreement with the NSF, has provided many in kind contributions for which the first author is grateful. Michelle Smith and Kimmerlee Johnson from Great Falls High School, Great Falls, Montana assisted in the data processing. We also thank the SSC folks for their hospitality during our visit. The TLRBSE Project

¹AE Aqr is a special case, however, as most of its far-IR emission is attributed to synchrotron emission.

is funded by the NSF under ESI 0101982 through the AURA/NSF Cooperative Agreement AST-9613615. This work makes use of data products from the Two Micron All Sky Survey, which is a joint project of the University of Massachusetts and IPAC/Caltech, funded by NASA and the NSF. CSB acknowledges support from the SSC Enhanced Science Fund, NASA’s Michelson Science Center, and the Spitzer Director’s Discretionary funds.

REFERENCES

- Abada-Simon, M., et al. 2005, *A&A*, 433, 1063
- Belle, K. E., Sanghi, N., Howell, S. B., & Holberg, J. B. 2004, *ApJ*, 128, 448
- Becklin, E. E., Farihi, J., Jura, M., Song, I., Weinberger, A. J., & Zuckerman, B. 2005, *ApJ*, 632, L119
- Brinkworth, C., et al. 2006, in preparation
- Cropper, M. 1990, *Space Science Reviews*, 54, 195
- Dubus, G., Campbell, R., Kern, R., Taam, R., & Spruit, H. 2004, *MNRAS*, 349, 869
- Farihi, J., Zuckerman, B., & Becklin, E. E. 2005, *Astronomische Nachrichten*, 326, 964
- Fazio, G., et al. 2005, *ApJS*, 154, 10
- Harrison, T. E., Howell, S. B., Huber, M., Osborne, H., Holtzman, J. A., Cash, J., & Gelino, D. 2003, *AJ*, 125, 2609
- Harrison, T. E., Howell, S. B., Szkody, P., Homeier, D., Johnson, J., & Osborne, H. 2004, *ApJ*, 614, 947
- Hinkle, K. H., Fekel, F. C., Joyce, R. R., Wood, P. R., Smith, V. V., Lebzelter, T. 2006, *ApJ*, in press (astro-ph/0512253)
- Howell, S. B., Nelson, L., and Rappaport, S. 2001, *ApJ*, 550, 897
- Howell, S. B., Harrison, T., & Szkody, P. 2004, *ApJ*, 602, L49
- Johnson, J. J., Campbell, R. K., Harrison, T. E., & Howell, S. B., 2005, *AAS*, 207, 7018
- Kolb, U. 1993, *A&A*, 271, 149
- Patten, B., et al. 2006, in preparation

- Rybicki, G., & Lightman, A. 1979, in *Radiative Processes in Astrophysics* (Berlin: Wiley-VCH)
- Spitzer, L. 1978, in *Physical Processes in the Interstellar Medium* (New York: John Wiley & Sons)
- Taam, R., & Spruit, H. 2001, *ApJ*, 561, 329
- Warner, B. 1995, in *Cataclysmic Variable Stars* (Cambridge: Cambridge University Press)
- Wickramasinghe, D., & Ferrario, L. 2000, *PASP*, 112, 873